Effects of the Third Order Transfer Maps and Solenoid on a High Brightness Beam

Zohreh Parsa
Physics Department
Brookhaven National Laboratory,
Upton, NY 11973

Abstract

We present a sketch of the formulation for obtaining Lie algebraic transfer maps for the solenoid through third order and its effect on the beam of charged particles. We discuss simulation results showing effects of solenoids on the laser driven high brightness photoelectrons for the proposed alternate injection system for Brookhaven Accelerator Test Facility.

I. INTRODUCTION

A brief overview of a Lie algebraic formulation is given in section II. Using Hamiltonian dynamics we describe the motion of a charged particle through electromagnetic fields. With Lie transformations we obtain the maps and trajectories for a particle along the beamline in a magnetic field (e.g. of solenoid). We discuss the transfer maps for magnetic elements and solenoid through third order and their effects on the beam of charged particles. In section III we discuss the effects of the solenoids used in the design of the proposed alternate injection system for the Brookhaven Accelerator Test Facility (ATF) [1].

II. FORMALISM

In this section we present an overview of the formalism used to obtain the trajectories of a particle along the beamline via Lie transformation. Using Maxwell's equations, axisymmetrical fields, and the relativistic equations for the charged particles motion along the beamline we can obtain the magnetic field components everywhere (e.g. of a solenoid given the on axis longitudinal component of the field $B_z = (B,0,0)$) and its effect on the particles motion.

We express the canonical equations in 2n-Dimensional phase space (e.g 6 Dim., in our calculation), as

$$\frac{d\psi_i}{dt} = [\psi_i, H], \qquad i = 1,2,\ldots 2n \tag{1}$$

and in terms of the Lie transformations as

$$\frac{d\psi_i}{dt} = -:H:\psi_i, \qquad i = 1,2,\ldots 2n \tag{2}$$

Where the Lie operator $(:H:)$ is generated by the Hamiltonian , (H), and Lie transformation,

$$M = e^{-t:H:}, \tag{3}$$

could generate the solution to Eq. (2) as

$$\psi_i = M\psi_i(0) \tag{4}$$

where ψ_i is the value of $\psi_i(t)$ at $t > 0$ and $\psi_i(0)$ is the initial trajectory. The interest is to find solutions to equations of motion which differ slightly from the reference orbit (e.g. the design orbit of an accelerator beamline. Design orbit for solenoid is along z-axis). Thus, we choose the canonical variables, from the values for the reference trajectory (for small deviations) and Taylor expand the Hamiltonian (H) about the design trajectory:

$$H = H_2 + H_3 + \ldots. \tag{5}$$

Where H_n is a homogeneous polynomial of degree n in the canonical variables. After transformations to the normalized dimensionless variables, we obtain the effective Hamiltonian H^{New}, expressed as

$$H^{\text{New}} = F_2 + F_3 + F_4 \ldots \tag{6}$$

Thus the particle trajectory $\vec{\psi} = (X, P_X, Y, P_Y, \tau, P_\tau)$ through a beamline element of length L can be described by

$$\psi_i^f = -:H^{\text{New}}:\psi_i, \qquad i = 1,2,\ldots 2n \tag{7}$$

The exact symplectic map that generates the particle trajectory through that element is,

$$M = e^{-L:H^{\text{New}}:}, \tag{8}$$

where, M describes the particle behavior through the element of length L. Using the factorization and expanding H^{New} as in Eq. (6), we obtain

$$M = e^{-L:H^{\text{New}}:} = e^{:f_2:}e^{:f_3:}e^{:f_4:}\ldots, \tag{9}$$

(for a map through 3rd order we need to include terms of f2, f3, and f4). Where $f_2 = LF_2$, $f_3 = LF_3$, $f_4 = LF_4$, etc.

To illustrate the above formalism, consider the evolution of the motion of particles in an external electromagnetic field described by the Hamiltonian

$$H = \sqrt{m^2c^4 + c^2\left[(p_x - qAx)^2 + (p_y - qA_y)^2 + (p_z - qA_z)^2\right]} + e\phi(x,y,z;t) \tag{10}$$

where m and q are the rest mass and charge of the particle, A and ϕ are the vector and scalar potentials such that $\vec{B} = \nabla \times \vec{A}$, $\vec{E} = -\nabla\phi - \nabla\vec{A}/\partial t$.

Making a canonical transformation from H to H_1 and changing the independent variable from time t to z (for convenience) for a particle in magnetic field (e.g. of solenoid) results in:

$$p_z = \left[(p_x - qAx)^2 + (p_y - qA_y)^2 + p_t^2/c^2 - m^2c^2\right]^{1/2}. \tag{11}$$

Where $H = -p_t$, $H_1 = -p_z$ and $t = (z/v_{0z})$ the time as a function of z. We next make a canonical transformation from H_1 to $H^{\rm New}$, with a dimensionless deviation variables (for convenience), $X = x/l$, $Y = y/l$, $\tau = c/l\,(t - z/v_{0z})$, $P_x = p_x/p_0$, $P_y = p_y/p_0$, $P_\tau = (p_t - p_0 t)/p_0 c.$, where l is a length scale (taken as 1 m in our analysis), with $\mathbf{P} = \vec{P}x + \vec{P}y$ and $\mathbf{Q} = \vec{X} + \vec{Y}$ defined as two dimensional vectors [3]. p_0 and p_0c are momentum and energy scales. Where p_0 is the design momentum, v_{0z} is the velocity on the design orbit and p_{0t} is value of p_t on the design orbit ($p_{0t} = \sqrt{m^2c^4 + p_0^2c^2}$) (reminding that design orbit for the solenoid is along the z-axis).

Thus, expanding the new Hamiltonian (eq.(6)) leads to:

$$F_2 = \frac{P_\tau^2}{(2\beta^2\gamma^2)} - \frac{1}{2}B_0\left(\vec{Q}\times\vec{P}\right)\cdot\hat{z} + \frac{1}{8}B_0^2Q^2 + \frac{P^2}{2} \tag{12}$$

$$F_3 = \frac{P_\tau^3}{(2\beta^3\gamma^2)} - \frac{P_\tau}{2\beta}B_0\left(\vec{Q}\times\vec{P}\right)\cdot\hat{z} + \frac{P_\tau}{8\beta}\left(B_0^2Q^2 + 4P^2\right) \tag{13}$$

$$\begin{aligned} F_4 = {} & \frac{P_\tau^4\,(5-\beta^2)}{8\beta^4\gamma^2} + \frac{P_\tau^2Q^2B_0^2\,(3-\beta^2)}{16\beta^2} \\ & - \frac{P_\tau^2}{2}\left(\vec{Q}\times\vec{P}\right)\cdot\hat{z}\,\frac{B_0\,(3-\beta^2)}{2\beta^2} \\ & + \frac{P_\tau^2}{2}\frac{P^2\,(3-\beta^2)}{2\beta^2} + \frac{Q^4}{16}\left(B_0^4 - 4B_0B_2\right)/8 \\ & + \frac{Q^2}{4}\frac{P^2\,3B_0^2}{4} + \frac{Q^2}{4}\left(\vec{Q}\times\vec{P}\right)\cdot\hat{z}\,\left(B_2 - B_0^3\right)/4 \\ & - \frac{1}{8}\left(\vec{P}\cdot\vec{Q}\right)^2B_0 - \frac{P^2}{4}\left(\vec{Q}\times\vec{P}\right)\cdot\hat{z}\,B_0 + \frac{P^4}{8} \end{aligned} \tag{14}$$

Following the hamiltonian flow generated by $H^{\rm New} = F_2 + F_3\ldots$ from some initial ψ_0 to a final ψ_f coordinates we can calculate the transfer map M (eq. 9) for the solenoid. Where F_2, F_3, and F_4 would lead to the 1st, 2nd, and 3rd order maps. The effects of which can be seen from eqs. (12-14). For example, the 2nd order effects due to solenoid transfer maps are purely chromatic aberrations (eq. 13). In addition to chromatic effects, we note the third order geometric aberrations (eq. 14). The coupling between X, Y planes produced by a solenoid is rotation about the z-axis which is a consequence of rotational invariance of the Hamiltonian $H^{\rm New}$ shown by eqs.(12-14), due to axial symmetry of the solenoid field.

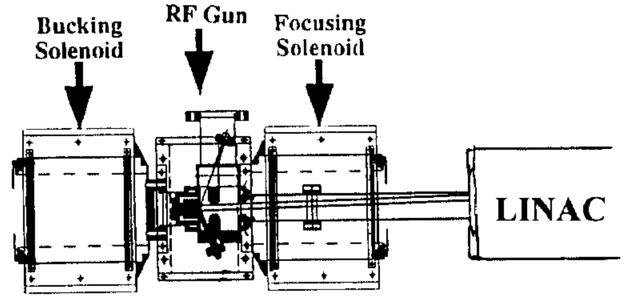

Figure 1: Sketch of the alternate injection system for ATF. A solenoid + gun + solenoid combination is placed straight ahead into the linac. (Not scaled).

For beam simulations, M can be calculated to any order using numerical integration techniques such as Runge-Kutta method depending on the computer memory and space available [3].

III. BNL ATF INJECTION SYSTEM

In this section we present some of our calculations and simulation results obtained for the proposed alternate (straight-ahead) injection system which consists of a pair of solenoids and an rf gun placed directly into the linac [1,7].

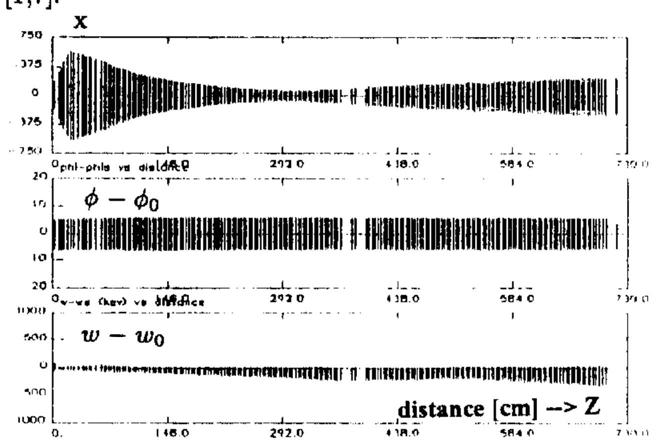

Figure 2: Shows the change in position x [cm], phase $\phi - \phi_0$ [degree] and energy $w - w_0$ [KeV] of particles at each element location, from the cathode through the linac exit. With solenoid current of 2140 A and $d = 62cm$ and $\sigma_r = .9mm$, $\sigma_z = 5ps$.

Present injection system consists of 2 sets of quadrupole triplets and a 180° achromatic double bend [1], where beam diverges quickly as it exits the gun and gets large as it traverses through the dipoles and the linac. We have used a pair of solenoids (placed before and after the gun such that B=0 on the cathode) shown in Fig. 1, which controls the beam divergence at the gun exit, reduces the emittance dilution due to space charge forces, and improves the conditions for production of high brightness low emittance beam needed e.g., for Free Electron Laser, and Inverse Free Electron Laser experiments. Figure 2 shows how the beam size increases as it drifts from the

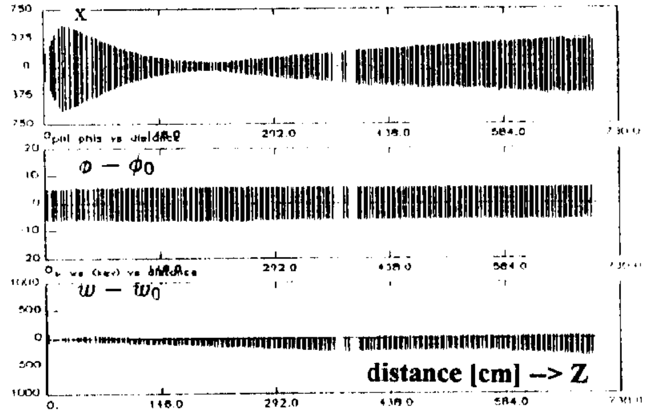

Figure 3: Shows the change in position x [cm], phase $\phi - \phi_0$ [degree] and energy $w - w_0$ [KeV] of particles at each element location, from the cathode through the linac exit. With solenoid current of 2180 A and $d = 62cm$ and $\sigma_r = .9mm$, $\sigma_z = 5ps$.

gun into the linac. The Beam converges to a waist in the linac resulting in a beam of smaller emittance at the linac exit which is of interest at ATF.

Comparison of Figs. 2 and 3 show locations of the beam waist and beam envelopes along the beamline from cathode through the linac. In Fig. 3, a 2% increase in the solenoid current resulted in the shift in the position of the beam waist in the linac and an emittance increase from ($\epsilon_x^{N,rms} = .278$, $\epsilon_y^{N,rms} = .243$) to ($\epsilon_x^{N,rms} = .390$, $\epsilon_y^{N,rms} = .333$) at the linac exit (as compared to Fig. 2). This illustrates the effects due to variation of the solenoid strength on the beam dynamics. In this analysis we used an initial E = 100 MV/m on the cathode, laser pulse length ($2\sigma_z$) of 10 ps, spot size $\sigma_r = 0.9mm$, initial phase of 43°, and d = 62 cm, (the distance from cathode to linac entrance). The solenoid for this design can vary up to 4.0 KG in strength. For example with a 2.2 KG solenoid strength we can preserve the beam quality and achieve high brightness, low emittance beam at the linac exit, which is needed for the FEL and laser acceleration experiments at ATF. With program PARMELA [6], with σ_r = 1mm and 0.9 mm (uniform beam distribution) we obtained beam emittance of few tenths of cm-mrad with energies of about $46MeV$ and brightness ($B = I^{peak}/\pi\epsilon_x^N\epsilon_y^N$) of orders of 10^{13} for the beam emerging from the exit of the linac.

IV. SUMMARY

We presented a sketch of the formalism used to obtain Lie algebraic maps through third order for magnetic elements e.g. a solenoid. Note that, the 2nd order aberration due to solenoid is purely chromatic. We discussed effects of solenoids used in the design of the alternate injection system for the ATF at Brookhaven National Lab. Where a pair of solenoids and an rf gun is placed directly into the linac, to improve the beam loss and the emittance growth at the linac exit (as may be with the present double bend system). With solenoid+gun+solenoid straight injection into the linac scheme we reduce the emittance dilution due to space charge forces, and produce the beam needed for FEL, IFEL and other laser acceleration experiments. We obtained small emittance (few tenths of cm-mrad) and high brightness of orders of 10^{13}. The solenoids used in the alternate injection system, controls the beam divergence at the gun exit, reduces the emittance dilution due to the space charge forces on the beam and produces a smaller beam emittance needed for the experiments at ATF.

V. REFERENCES

*Work performed under the auspices of the U.S. Department of Energy, Contract Number DE-ACO2-76-CH00016.

1. Z. Parsa, *"Development of the Alternate Entry Port for the ATF"*, Proc. IEEE May 17-20 PAC, Washington D.C. (1993).
2. Z. Parsa, *"Lie Algebraic Transfer Maps of Magnet System and Nonlinear Aberrations in the Beam"*, BNL Tech. Note ADD/CAP/TN 5 (1/21/89) and References therein. Additional Lie transfers maps for drifts, quadrupole, dipole etc. were included in this reference.
3. A. Dragt, Program MARYLIE, Private comm.; ibid *"Numerical third-order transfer map for solenoid "*, NIM, A298 (1990), and References therein. MARYLIE includes 3rd order maps for solenoid with soft-edge "bump" function model for the field. We thank A.Dragt for discussions and providing his code. We did not include any results with MARYLIE for our analysis of the ATF alternate injection system with solenoids, since this code does not provide acceleration through the rf gun and the linac. Results with MARYLIE for the beamline without rf and linac accelerations will be given in a separate note.
4. Z. Parsa, *"Preliminary Emittance Measurements and Calculations of the Laser Excited Beam from the BNL Accelerator Test Facility Radio Frequency Electron Gun"*, Vol.II, Sec.II, p1–54, BNL-52292 (1991) and References therein; K. McDonald *et al.*, Proc., EPAC88, June (1988); K. Batchelor *et al.*, *"Operational Status of Brookhaven Accelerator Test Facility"*, Proc. 1989 IEEE Particle Accelerator Conf. Chicago, Ill, March 20–23, 1989, #89CH2669-0 (1990).
5. Z. Parsa, *"On Beam Emittance and Invariants - Applications to ATF Beamline"*, Proc. 2nd EPAC, Nice - France, Nile Ed., Frontiers, (1990); BNL Report BNL-44364 (1990) and Ref. therein.
6. Z. Parsa, and L. Young, *"The BNL Photocathode Gun with the Code PARMELA"*, Nucl. Inst. & Meths. A318; BNL-46804 (1991); L. Young, (Private comms.), PARMELA (1993 version).
7. Z. Parsa, *"An Alternate Injection System for the BNL Accelerator Test Facility"*, BNL-48403, APS April 12-15, Washington D.C. (1993).